REPUBLIC OF TURKEY

YILDIZ TECHNICAL UNIVERSITY

GRADUATE SCHOOL OF SCIENCE AND ENGINEERING

DESIGN OPTIMIZATION OF RAILGUN'S ELECTROMAGNETIC FORCE USING SURROGATE MODELLING TECHNIQUES

Habil Akansel AKYOL

MASTER OF SCIENCE THESIS

Department of Electronics and Communication Engineering

Communication Engineering Program

Supervisor

Prof. Dr. Ahmet KIZILAY

February, 2022

REPUBLIC OF TURKEY

YILDIZ TECHNICAL UNIVERSITY

GRADUATE SCHOOL OF SCIENCE AND ENGINEERING

DESIGN OPTIMIZATION OF RAILGUN'S ELECTROMAGNETIC FORCE USING SURROGATE MODELLING TECHNIQUES

A thesis submitted by Habil Akansel AKYOL in partial fulfillment of the requirements for the degree of MASTER OF SCIENCE is approved by the committee on 09.02.2022 in Department of Electronics and Communication Engineering, Communication Engineering Program.

Prof. Dr. Ahmet KIZILAY
Yıldız Technical University
Supervisor

Approved By the Examining Committee

Prof. Dr. Ahmet KIZILAY, Supervisor
Yildiz Technical University _____

Doç.Dr. Hamid TORPİ, Member
Yildiz Technical University _____

Doç.Dr. Peyman MAHOUTİ, Member
Istanbul University-Cerrahpasa _____

I hereby declare that I have obtained the required legal permissions during data collection and exploitation procedures, that I have made the in-text citations and cited the references properly, that I haven't falsified and/or fabricated research data and results of the study and that I have abided by the principles of the scientific research and ethics during my Thesis Study under the title of Design Optimization of Railgun's Electromagnetic Force Using Surrogate Modelling Techniques supervised by my supervisor, Prof. Dr. Ahmet KIZILAY. In the case of a discovery of false statement, I am to acknowledge any legal consequence.

Habil Akansel AKYOL

Signature

Dedicated to my family

and my best friends

ACKNOWLEDGEMENTS

Firstly, I would like to thank my advisor Prof. Ahmet KIZILAY for the enthusiasm, energy and motivation throughout my academic life. He is very kind, inspiring and supportive mentor. It has been an honor to be his student.

I would like to thanks to the many friends, colleagues who had helped me during my researches and writing of my thesis and to the Tractus Technology, the data science company I am currently working for, for providing all kinds of support during this process.

I would like to thank the Istanbul Naval Shipyard, ASELSAN A.Ş and LEONARDO SpA Company for their supports, trainings and demonstrations of regarding to the weapon systems.

Special thanks to my wife, Zübeyde, who has supported and helped me, discussed ideas and also prevented several wrong turns.

Finally, I would like to thanks my parents for supporting me, and being with me throughout my education life.

Habil Akansel AKYOL

TABLE OF CONTENTS

LIST OF SYMBOLS vii
LIST OF ABBREVIATIONS viii
LIST OF FIGURES ix
LIST OF TABLES x
ABSTRACT xi
ÖZET xiii
1 INTRODUCTION 1
1.1 Literature Review 1
1.2 Objective of the Thesis 2
1.3 Hypothesis 2
2 ANALYSIS OF DIFFERENT RAILGUN GEOMETRIES 4
2.1 Railgun Theory 4
2.1.1 Related Equations 4
2.1.2 Inductance Gradient Calculation with Kerrisk's Method 7
2.2 Simulation Model Parameters 8
2.2.1 Geometry 9
2.2.2 Rail and Armature Materials 11
2.2.3 Input Current and Distributions 12
2.3 Simulation Results 12
3 SURROGATE MODELLING 17
3.1 What is Surrogate Modelling 17
3.2 Types of Surrogate Models 17
3.2.1 Supervised and Unsupervised Learning 17
3.2.1.1 Regression and Classification 18
3.3 Surrogate Model Techniques Used in This Thesis 19
3.3.1 Artificial Neural Networks 19
3.3.2 Support Vector Regression 20
3.3.3 Random Forests 22
3.3.4 XGBoost 22
3.3.5 K-Nearest Neighbors 23
3.3.6 Multi Linear Regression 23

4 RAILGUN'S ELECTROMAGNETIC FORCE USING SURROGATE MODELLING TECHNIQUES **25**

5 PARTICLE SWARM OPTIMIZATION **36**

6 RESULTS AND DISCUSSION **38**

REFERENCES **40**

PUBLICATIONS FROM THE THESIS **45**

LIST OF SYMBOLS

q	Charged Particles
$\vec{I}$	Current
$\vec{J}$	Current Density
$\overrightarrow{V_d}$	Drift Velocity
$\vec{J}_e$	Eddy Current
$\vec{E}$	Electrical Field
L'	Inductance Gradient
$\vec{F}$	Lorentz Force
$\vec{H}$	Magnetic Field Intensity
$\vec{B}$	Magnetic Flux Density
$\vec{A}$	Magnetic Vector Potential
μ	Permeability
μ_0	Permeability of Free Space
r	Radial Distance

LIST OF ABBREVIATIONS

AI	Artificial Intelligence
ANN	Artificial Neural Network
FEM	Finite Element Method
KNN	K-Nearest Neighbors
MHA	Meta-Heuristic Algorithms
MLR	Multiple Linear Regression
OLS	Ordinary Least Squares
PSO	Particle Swarm Optimization
RMSE	Root Mean Square Error
SMAPE	Symmetric Mean Absolute Percentage Error
SVMs	Support Vector Machines
SVR	Support Vector Regression

LIST OF FIGURES

Figure 2.1 Railgun diagram 4
Figure 2.2 Current - magnetic field and Lorentz Force relation 5
Figure 2.3 Produced magnetic field 6
Figure 2.4 Geometrical parameters in Kerrisk's method 8
Figure 2.5 Rail geometries 9
Figure 2.6 Armature geometries 10
Figure 2.7 Current density graph of half-cylindrical rail - C type armature pair 12
Figure 2.8 Inductance gradient graph of C type armature 13
Figure 2.9 Inductance gradient graph of rectangular type armature 14
Figure 2.10 Inductance gradient graph of hollow type armature 14
Figure 3.1 An example of neural network structure 20
Figure 3.2 Illustrative example of SVR 21
Figure 4.1 Railgun geometric variables 25
Figure 4.2 Prediction graph of ANN method 33
Figure 4.3 Prediction graph of SVR method 33
Figure 4.4 Prediction graph of Random Forests method 34
Figure 4.5 Prediction graph of KNN method 34
Figure 4.6 Prediction graph of MLR method 35
Figure 4.7 Prediction graph of XGBoost method 35

LIST OF TABLES

Table 2.1 Kerrisk's constants 8
Table 2.2 Armature properties (cm) 11
Table 2.3 Rail properties (cm) 11
Table 2.4 Average inductance gradient values (uH/m) 15
Table 4.1 Geometric variables and dataset inputs 26
Table 4.2 Some examples of dataset 26
Table 4.3 Model tuning parameters 28
Table 4.4 Prediction results 32
Table 5.1 Optimization results 37

ABSTRACT

Design Optimization of Railgun's Electromagnetic Force Using Surrogate Modelling Techniques

Habil Akansel AKYOL

Department of Electronics and Communication Engineering

Master of Science Thesis

Supervisor: Prof. Dr. Ahmet KIZILAY

Electromagnetic output force is used for evaluating the performance and the effectiveness of a railgun which is highly depended on the Railgun geometric design parameters. This thesis has aimed to provide an Artificial Intelligence based surrogate model for a railgun design to prevent time consumption at simulation and analysis stages and to make design optimization process computationally efficient. For this reason, three different rail geometries have been combined and simulated with three different armature types by using Ansys Maxwell which is based on 3-D Finite Element Method (FEM). Within the scope of this study; first of all, according to the efficiency one of the best rail and armature pair was selected. Secondly, a dataset with inputs and outputs was created by changing the geometric variables of the selected pair. Thirdly, using this dataset; six different surrogate models were trained, tuned and tested. Railgun's output force was predicted with these models. Finally, in order to obtain railgun's geometric inputs for a specific output force, Particle Swarm Optimization (PSO) was carried out with the surrogate model that giving the best result. These optimization results were compared with the Ansys simulation outputs and found to be hand to hand. Thus, herein, a computationally

efficient method for design optimization of railgun designs has been achieved using surrogate-based modelling techniques.

Keywords: Surrogate modelling, optimization, railgun, artificial neural networks

ÖZET

RAILGUN'IN ELEKTROMANYETİK KUVVETİNİN TEMSİLİ MODELLEME TEKNİKLERİYLE TASARIM OPTİMİZASYONU

Habil Akansel AKYOL

Elektronik ve Haberleşme Mühendisliği Anabilim Dalı

Yüksek Lisans Tezi

Danışman: Prof. Dr. Ahmet KIZILAY

Elektromanyetik silah olarak da adlandırılan Railgun'ın elektromanyetik çıkış gücü silahın geometrik tasarım parametrelerine büyük ölçüde bağlıdır ve bu güç elektromanyetik silahın performansını ve etkinliğini değerlendirmek için kullanılır. Bu tez, simülasyon ve analiz aşamalarında zaman kaybını önlemek ve tasarım optimizasyon sürecini verimli hale getirmek için bir elektromanyetik silah tasarımı için Yapay Zeka tabanlı bir temsili (surrogate) model sağlamayı amaçlamıştır. Bu kapsamda, 3 Boyutlu Sonlu Elemanlar Metodu ile hesaplama yapan Ansys Maxwell programı kullanılarak üç farklı ray geometrisi ile üç farklı armatür tipinin kombinasyonel birleşimleri simüle edilmiştir. Simülasyonlar neticesinde; öncelikle verimliliğe göre en iyi ray ve armatür çiftlerinden biri seçilmiştir. İkinci olarak, seçilen ray armatür çiftinin geometrik dizayn parametreleri değiştirilerek girdileri ve çıktıları olan bir veri seti oluşturulmuştur. Sonrasında bu veri seti altı farklı temsili model ile eğitilmiş, geliştirilmiş, test edilmiş ve silahın çıkış kuvveti tahmin edilmiştir. Son kısımda ise belirli bir elektromanyetik çıkış kuvvetine ulaşmak için silahın geometrik değişkenlerinin neler olması gerektiğini bulmak amacıyla, en iyi sonucu veren temsili model ile Parçacık Sürüsü Optimizasyonu (PSO) yöntemi

birlikte kullanılarak bir optimizasyon gerçekleştirilmiştir. Bu optimizasyon sonuçları, Ansys simülasyon çıktıları ile karşılaştırılmış ve birebir olduğu görülmüş, temsili modelleme teknikleri kullanılarak elektromanyetik silah tasarımlarının tasarım optimizasyonu için hesaplama açısından verimli bir yöntem elde edilmiştir.

Anahtar Kelimeler: Temsili modelleme, optimizasyon, elektromanyetik silah, yapay sinir ağları

1
INTRODUCTION

1.1 Literature Review

Conventional weapons, which are currently widely used, work with gunpowder or explosive propellant. Therefore, there are explosion risks during usage of the weapons and storage of the projectiles. If the projectile is stuck in the barrel and cannot be removed properly, it may explode and cause loss of life and property. Nowadays, we often see this painful news, events frequently.

Because of the including explosive material, if the projectile is not stored under suitable conditions such as humidity or temperature, it cannot be fire. Projectile loses firing conditions. Since the projectile is triggered by electrical energy and no explosive is used, electromagnetic weapons or launchers is safer than conventional weapons. Another advantage of electromagnetic weapons to the conventional weapons is that they can reach longer ranges and higher velocities with high kinetic energy.

Electromagnetic weapons also have two major disadvantages. The first is that it cannot be used in vehicles where weight is important, such as aircraft, because it requires high-dimensional and heavy energy units. For this reason, electromagnetic launchers are used on naval ships or ground-mounted fixed locations. The second disadvantage is that due to the long charging and discharging times, it is necessary to wait for a certain time for each firing and therefore the fire rate is low.

In order to design the most effective railgun, we need to analyze railgun key parameters such as magnetic flux density between the rails, maximum current density over the rail cross section, repulsive force acting on the rails, and inductance gradient of the rail. These parameters affect output force of the railgun, that's why it needs to be understood that how these key parameters react under different boundary conditions and variation in dimensions [1].

The evaluation of these parameters during the firing is uneasy and costly. Therefore, regarding simulations should be done before the production. In recent years, many studies had been carried out for creating surrogate models using Artificial Intelligence (AI) algorithms with high computationally efficiency to be used in design optimization or design with high performance and accuracy requirements [2-3]. Some studies published in the literature in the field of surrogate based modeling of high-frequency electromagnetic devices can be mentioned: modelling of microwave transistors [4-8], reflection phase characteristic prediction of reflect array antennas unit elements [9-12], for synthesis and analysis of microstrip lines [13-14], for modelling a microstrip patch designs [15-17], dielectric properties prediction of the vegetation [18], investigation the effects of aperture dimension ratio on electrical shielding effectiveness [19] and prediction of the radiated emission from heatsink's and heatsink optimization [20].

On the optimization side, Meta-Heuristic Algorithms (MHA) has been widely used as an powerful solution method for finding optimal results in design optimization process of many microwave devices [21-32] as well. Due to their unique heuristic search methods, these algorithms can be used in for solving non-differentiable or discontinuous, non-convex problems. Also, they are used for solving nonlinear problems that might not be solved with gradient based algorithms [3].

1.2 Objective of the Thesis

Product design in engineering is mainly based on a comprehensive analysis of product performance under various design parameters. These analyzes are most often executed through time-consuming computer simulations. This thesis has aimed to provide an Artificial Intelligence based surrogate model for a railgun design to prevent time consumption at design and simulation stages and to make design optimization process computationally efficient.

1.3 Hypothesis

Using AI based surrogate model, it is sufficient to give only the railgun's geometrical inputs to see the railgun's electromagnetic force without drawing geometry and running simulation again and again. Considering that hundreds of parameters are

changed while making a design, surrogate model saves a lot of time. As an example design optimization study case, one of the commonly used MHA algorithms Particle Swarm Optimization (PSO) can be used for data driven surrogate model assisted optimization process. Thus, by using AI based computational efficient surrogate modelling and Meta-Heuristic optimization algorithms; a fast, reliable, accurate and computational efficient optimization process can be achieved.

2
ANALYSIS OF DIFFERENT RAILGUN GEOMETRIES

2.1 Railgun Theory

The railgun consists of two parallel conductors called rails which connected each other by a non-ferromagnetic material called armature that is also carriers of the projectiles. While the current flows through the parallel rails, it generates a magnetic field according to the right-hand rule, with the magnetic field lines vertical to the rails and the armature. These magnetic field lines and the current flowing along the armature produce a force. This force is called Lorentz force. Lorentz force triggers the armature throughout the rails. [33]. A simple diagram of a railgun and Lorentz force are shown in Figure 2.1 below.

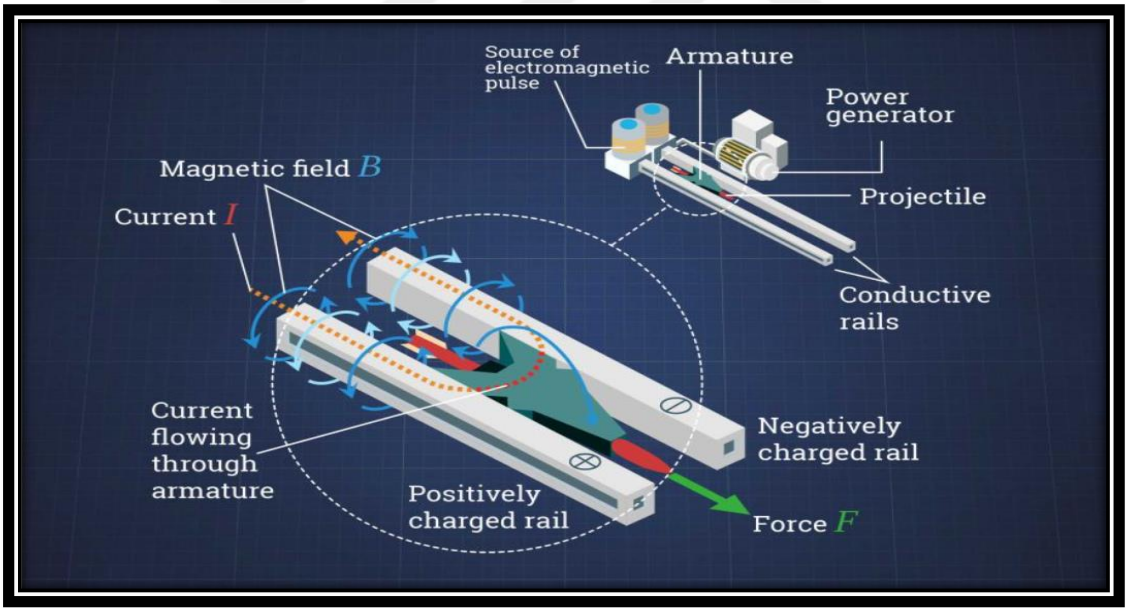


Figure 2.1 Railgun diagram [34]

2.1.1 Related Equations

The Lorentz force is written as:

$$\vec{F} = q(\overrightarrow{V_d} \times \vec{B}) \tag{2.9}$$

Armature between the rails completes the circuit path, current flows through rails

and armature with a velocity $\overrightarrow{V_d}$. A magnetic field $(\vec{B})$ between the rails is also created since the flowing current through the rails. Velocity of the current and magnetic field vectors create a force $(\vec{F})$ on charged particles (q) between the rails. Figure 2.2 shows this relation in below [1] [35].

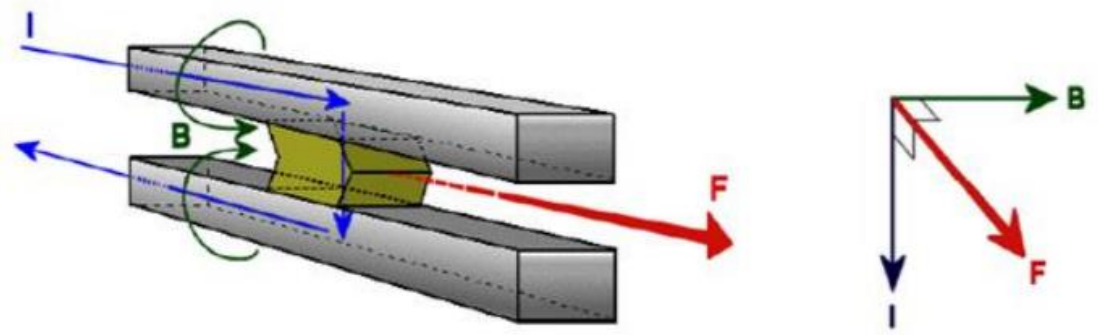


Figure 2.2 Current - magnetic field and Lorentz Force relation [35]

The magnitude of the Lorentz force can be written as:

$$\vec{F} = q(|\overrightarrow{V_d}|\,|\vec{B}|) \tag{2.10}$$

where q is charge, $\overrightarrow{V_d}$ is the velocity of the charge, and $\vec{B}$ is the magnitude of the magnetic field generated between the rails. The amount of charge passing through the armature can be formulated as [35];

$$q = It \tag{2.11}$$

where I is the current and t is the elapsed time of a charge with a velocity of $\overrightarrow{V_d}$ through the armature having a length of l. Now, Equation 2.11 can be written as;

$$q = I\frac{l}{V_d} \tag{2.12}$$

Substituting q in Equation 2.10 using Equation 2.12, Lorentz force can be written as;

$$\vec{F} = \vec{B}Il \tag{2.13}$$

Differentiating Equation 2.13 along the armature height l yields the following equation;

$$d\vec{F} = \vec{B}I\,dx \tag{2.14}$$

The current flowing through a semi-infinite straight wire generates a magnetic field $\vec{B}$. This magnetic field can be stated by Biot-Savart Law as below;

$$\vec{B} = \frac{\mu_0 I}{4\pi r} \tag{2.15}$$

Where the constant μ_0 is permeability of free space and r is the radial distance from the center of wire.

Now, in this case we have to assume two things. First one is that the current flows only through the center of the rails, the second one is that the magnetic features of the rails are similar to the features of long circular wires [33]. This situation is shown in Figure 2.3;

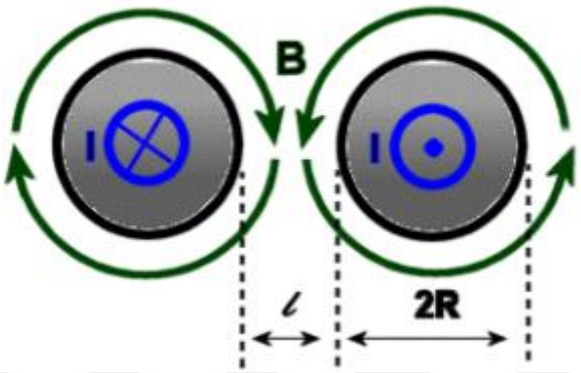


Figure 2.3 Produced magnetic Field [35]

Applying the Equation 2.15 into Equation 2.14 and integrating it, Lorentz force is written as;

$$F = \frac{\mu_0 I^2}{4\pi} \int_R^{R+l} \left(\frac{1}{x} + \frac{1}{2R + l - x} \right) dx \tag{2.16}$$

Where x is a point between the center of rails. With the evaluating the integral yields, Equation 2.16 becomes;

$$F = \frac{\mu_0 I^2}{4\pi} \ln \left\{ \frac{(R + l)^2}{R^2} \right\} \tag{2.17}$$

After this, we can consider the right side of the Equation 2.17 as two parts. First part is I^2 and second part is the rest the right side except I^2. The second part is called inductance gradient (L'). It is a magnetic field factor that depends solely on the geometry of the railgun. Its unit is H / m. L' is written as;

$$L' = \frac{\mu_0}{4\pi} \ln\left\{\frac{(R+l)^2}{R^2}\right\} \tag{2.18}$$

Here, we can easily see that the inductance gradient depends on the railgun's geometric variables.

Substituting Equation 2.18 into 2.17 gives the Lorentz Force formula, but it is predicted that exactly half of the electromagnetic energy is used to store energy in the magnetic field along the rails and the other half is used used to supply kinetic energy to the armature [36]. Consequently, the Lorentz Force is written as;

$$F = \frac{1}{2} L' I^2 \tag{2.19}$$

2.1.2 Inductance Gradient Calculation with Kerrisk's Method

As it is seen from the equations in above that inductance gradient is a function of railgun dimensions and the rail material, also a useful parameter that used to show the efficiency of the railgun. Therefore, there are many studies on the effects of rail and armature geometry [37], [38], [39] and materials [40] on the inductance gradient. In this scope, Kerrisk has proposed an analytical L' formula based on the field calculations in two-dimensional geometry. In that study, Kerrisk assumes four main points; First one is that the rails of the railgun are very long, second one is that rails are rectangular, third one is that the rails' corners are rounded, and the last one is that current flows only on the rail surface [41].

Kerrisk's proposed method regarding to the calculation of the inductance gradient has include the geometrical variables regarding to the railgun and some constants regarding to the materials. Kerrisk's proposed formula is given below [33], [37];

$$L' = [A + B \ln(a_1 \frac{w}{h} + a_2 \frac{w}{h}\frac{s}{h})] \ln\left(b_1 + b_2 \frac{s}{h} + b_3 \frac{s}{h} + b_4 \frac{s}{h}\frac{w}{h}\right) \tag{2.20}$$

where w is rails' width, s is the length of interval between the rails and h is rail height. Figure 2.4. shows these geometrical parameters. And the constants in the Kerrisk's proposed formula are shown in Table 2.1.

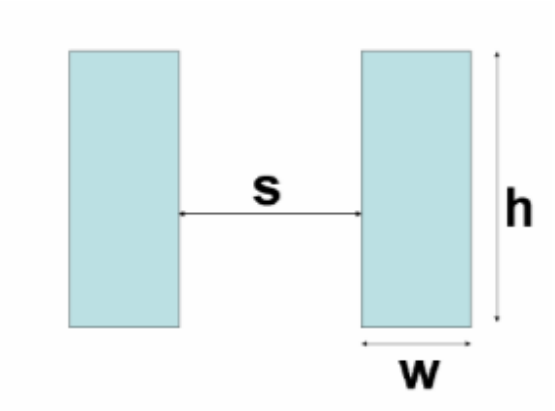


Figure 2.4 Geometrical parameters in Kerrisk's method [33]

Table 2.1 Kerrisk's constants

a_1	3.397143
a_2	-0.06603
b_1	1.007719
b_2	2.743651
b_3	0.022093
b_4	0.263739
A	0.44061
B	-0.0771

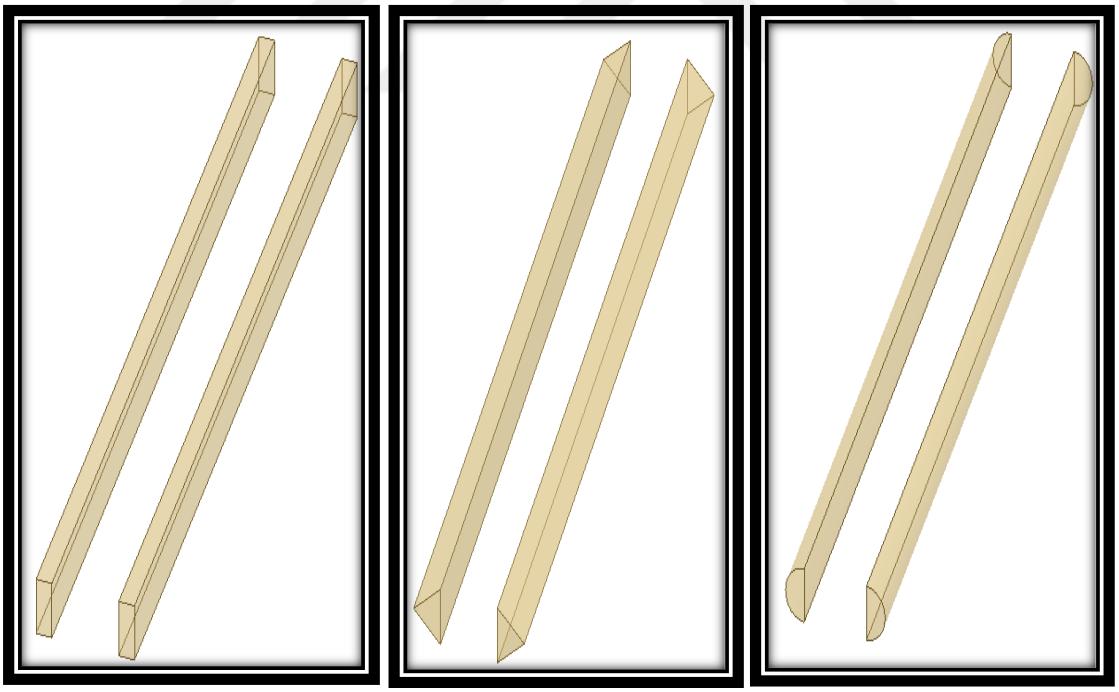
2.2 Simulation Model Parameters

In order to analyze effects of railgun geometry on output force, all simulation parameters have been taken equal at all simulations except geometry variations.

2.2.1 Geometry

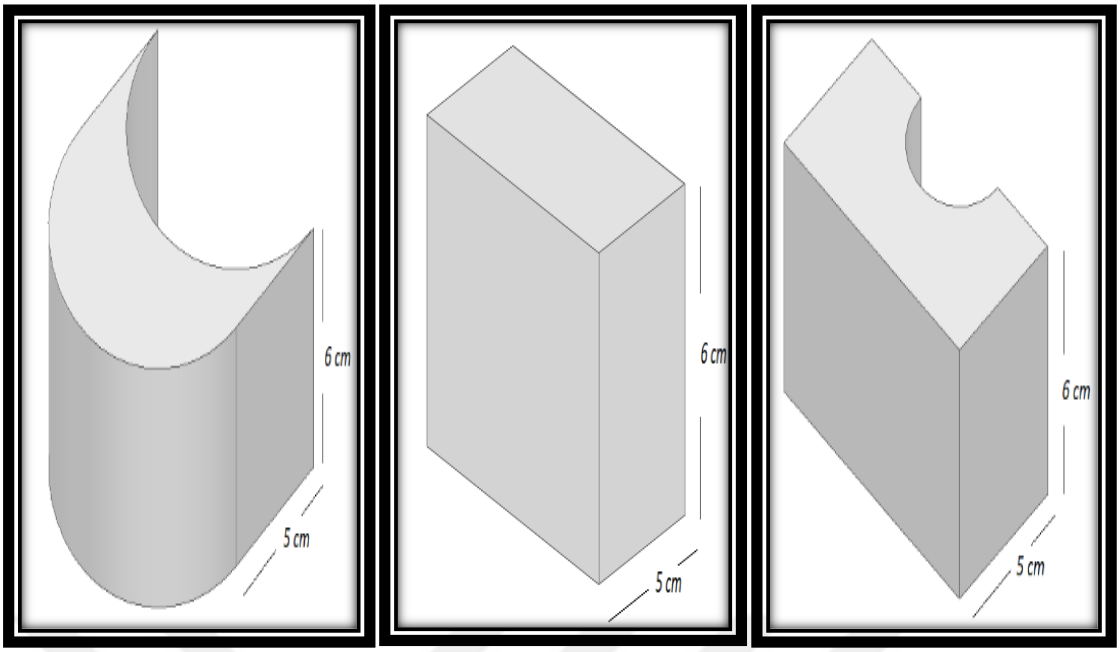
Square, triangular and half-cylindrical rails were selected as different rail geometries. C type, rectangular and hollow types of armature geometries were selected as different armature geometries. Inner side of the rails are preferred flat shape because of its advantages such as high inductance gradient, easy cleaning, easy maintenance, easy removing, easy loading, lower cost and uniform field distribution [37]. The rail pairs have been shown below in Figure 2.5.

There are many armature design studies in the literature and the industry, but the most common and most studied designs are C-type armatures and brush armatures [42-43]. For this reason, in this study C-type armature was chosen firstly for analysis. Secondly, a rectangular armature with the same volume as the C-type was designed to examine the volume effect. Lastly, a hollow-type armature which is between C-type and rectangular geometry as a similarity was designed to examine the surface area effect. The armature geometries have been shown below in Figure 2.6.



a. Rectangular rail **b.** Triangular rail **c.** Half-cylindrical rail

Figure 2.5 Rail geometries



a. C type armature **b.** Rectangular type **c.** Hollow type armature

Figure 2.6 Armature geometries

Rail material has been chosen copper; armature material has been chosen aluminum. Each rail has 100 cm length, 6 cm height and equal rail cross section which is adjusted according to the half cylindrical rail radius (r = 3 cm). Railgun calibrations are designed equally; rail separations were fixed to 10 cm and each armature's width was fixed to 10 cm for creating a conduction path between rails. Armature height is taken 6 cm that is equal to the rail height.

In order to observe whether surface area and volume has an effect on the output force, C type armature and rectangular armature types were designed with equal volumes ($300cm^3$), as hollow and rectangular types have equal surface area ($280cm^2$).

Since the three different rail geometries will be combined with the three different armature types, a total of nine different railgun structure will be observed. The detailed armature and rail design properties are shown in Table 2.2 and Table 2.3 respectively below.

Table 2.2 Armature properties (cm)

Armature type	Rail intersection	Height	Surface area	Volume
C type	5	6	348.5	300
Rectangular	5	6	280	300
Hollow	5	6	280	255

Table 2.3 Rail properties (cm)

Rail type	Length	Height	Rail cross section	Surface area	Volume
Cylindrical	100	6	14.13	1570	1413
Rectangular	100	6	14.13	1700	1413
Triangular	100	6	14.13	1745	1413

2.2.2 Rail and Armature Materials

Inductance gradient depends on the material as well as the geometry. Therefore, we can say there is a direct connection between the performance and the material of railgun. Besides material effects the cost, lifetime, reliability and quality of railgun. According to high Roche quality factor of materials; rail material is commonly selected the copper alloy or composites. Armature material is selected aluminum [44]. Therefore, in this study rail material has been chosen copper, armature material has been chosen aluminum.

2.2.3 Input Current and Distributions

Skin effect causes gaps on the material, these gaps are able to result in high-voltage drain and ablation on the surface of armature and rails [45]. Uniformity of the current distribution reduces the harmful effect of the skin effect effectively. Material and thickness of the railgun effect the current distribution and uniformity on the rails. Creating railgun material using thin layers increases the uniformity, reduces the harmful effects [46]. Based on advances in uniformity studies and since we want to examine only the effect of geometry variations on the output force, input current was adjusted 100 kA as a constant value along the rails. Thus, because of the constant input current, output force and inductance gradient have the same effect on evaluating the railgun's performance (Equation 2.19).

Current density graph of Half-cylindrical rail - C type armature pair has been given below in Figure 2.7 as an example.

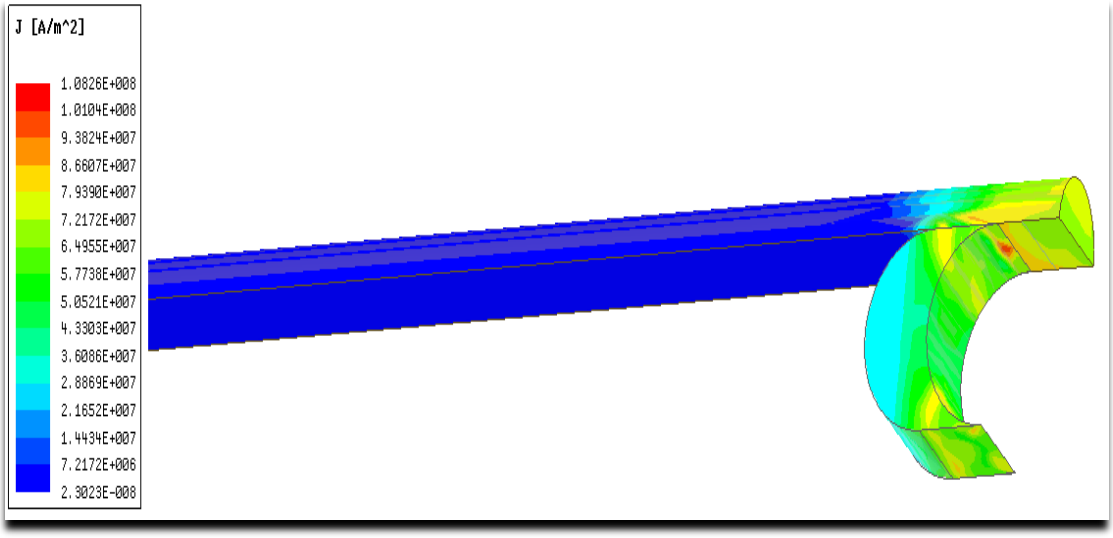


Figure 2.7 Current density graph of half-cylindrical rail - C type armature pair

2.3 Simulation Results

Ansys Maxwell simulation software allows us to 2D and 3D low frequency electric field simulation for analysis of electromechanical and electromagnetic systems.

Three rail geometries have been simulated three different armature types, totally nine different cases were observed. Armatures were moved parametrically along

the rails and calculations have been carried out by using ANSYS software that based on 3-D Finite Element Method (FEM). FEM is a numerical technique that divides the modeled geometry to the finite elements and solves the problem partially. In analysis, surface approximation-based mesh structure was selected for Half-cylindrical rail and length-based mesh structure was selected for other armature and rail geometries. Same amount of mesh cells was used for the same geometry in different simulations.

The inductance gradient has been calculated for each scenario, armature dependent graphics for each rail has been shown in Figure 2.8, 2.9, 2.10 respectively.

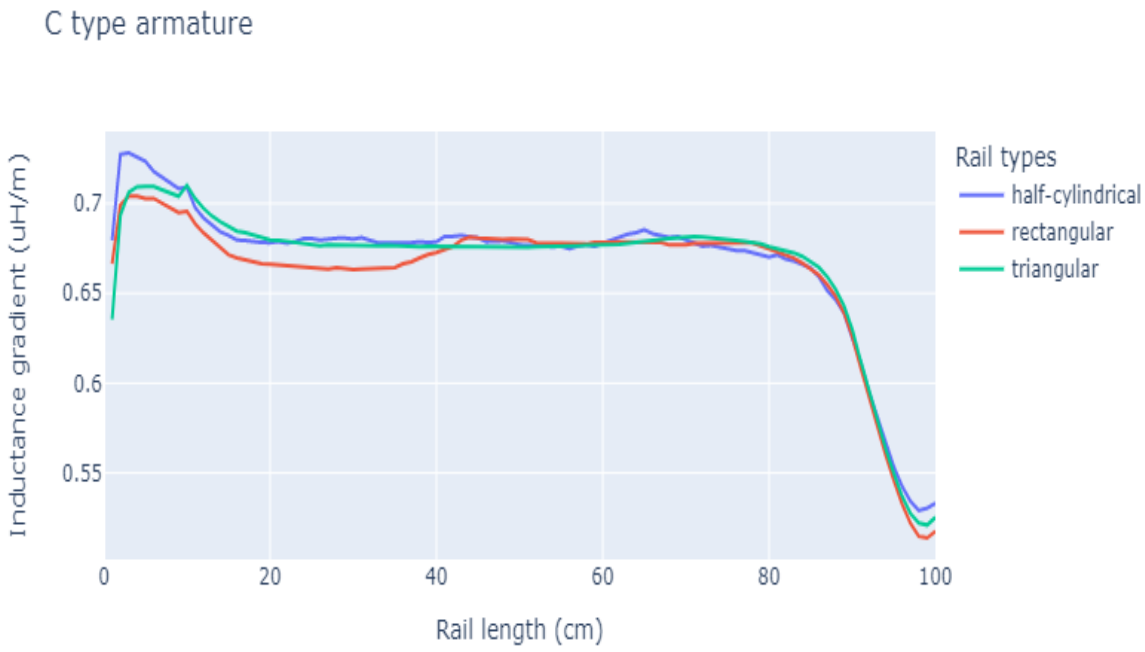


Figure 2.8 Inductance gradient graph of C type armature

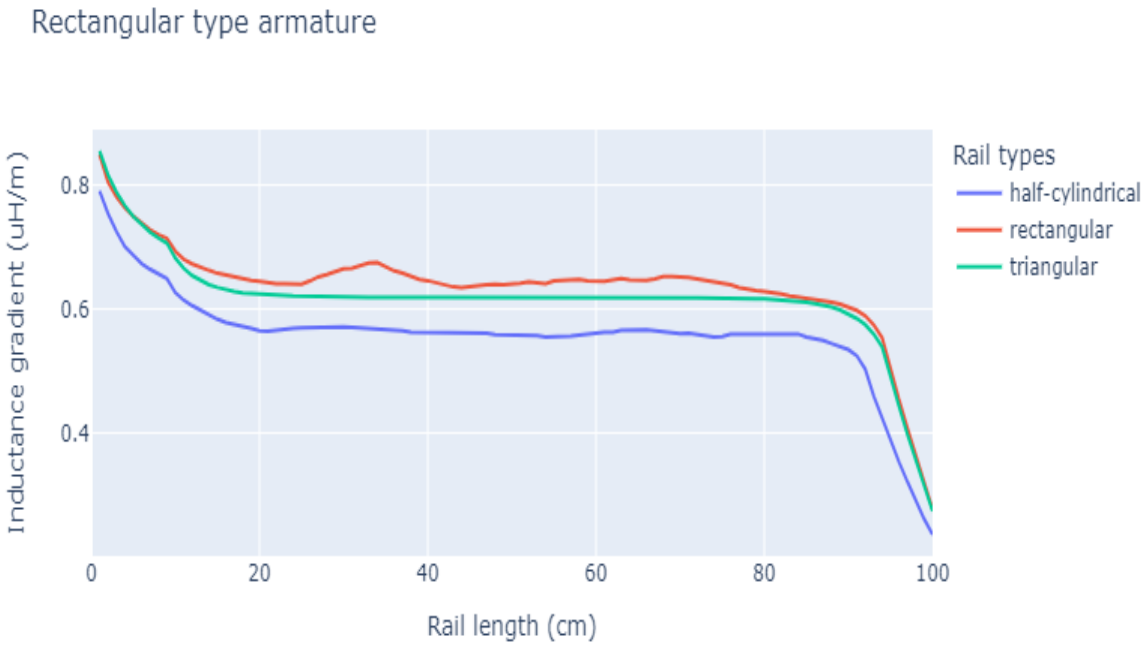


Figure 2.9 Inductance gradient graph of rectangular type armature

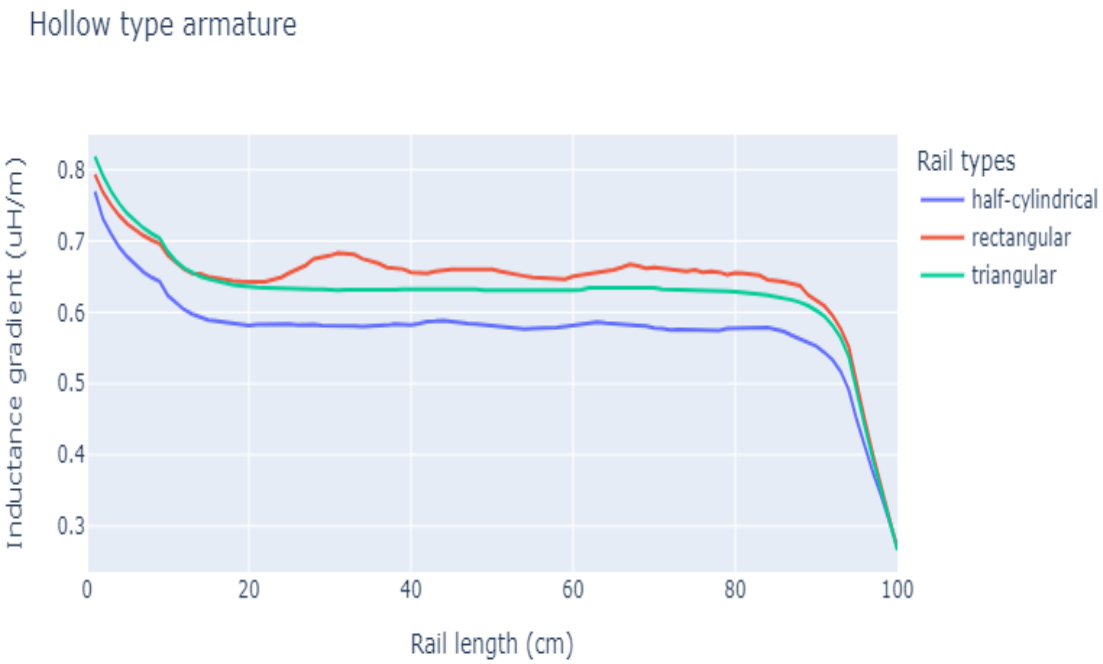


Figure 2.10 Inductance gradient graph of hollow type armature

It is seen from Figure 2.8, 2.9 and 2.10 that inductance gradient values directly dependent the rail-armature geometry. The output force of the triangular rail geometry is stable and does not fluctuate along the rails while rectangular and cylindrical rail geometry fluctuates.

The average of inductance gradient values regarding to the armature-rail pairs are shown in Table 2.4.

Table 2.4 Average inductance gradient values (uH/m)

Armature type	**Half-cylindrical rail**	**Rectangular rail**	**Triangular rail**
C type	0.68	0.67	0.68
Rectangular	0.57	0.65	0.62
Hollow	0.58	0.65	0.63

Due to the skin effect, current passes on the exterior surfaces of the conductors during the first period of launch. And in the following launch period, due to the velocity skin effect (VSE) current is concentrated on the exterior surface again [42]. Since all rails' inner surfaces where the current flows [45] to the armature are the same, the armature with a large surface area is expected to provide better inductance gradient.

As seen in Table 2.4, Half-cylindrical rail-C type armature and Triangular rail- C type armature pairs have same inductance gradient value of 0.68. This value is maximum among the others. On the other hand, Half-cylindrical rail-C type armature pair has minimum inductance gradient value of 0.58. There is 0.1 interval between minimum and maximum inductance gradient values. This corresponds to an efficiency difference of 10%, which is very important to observe before the production phase.

As seen in Table 2.4, C type armature has the highest inductance gradient for all cases. When the inductance gradient is evaluated in terms of surface area; C-type

armature with high surface area has given better inductance gradient in all situations. Rectangular and hollow type armatures with same surface area as each other but with a lower surface area than C type armature have given the same inductance gradient with each other but lower than C type armature.

Between the C-type and rectangular type armatures with the same volume but different surface areas; C type with a high surface area has given higher inductance gradient. Besides, between the rectangular and hollow type armatures with the same surface area but different volumes; they have given almost same inductance gradient.

Also, it is seen that from Table 2.4, the same armature type gives different inductance gradient values in combination with different rail types, so we can say that not only the armature geometry, but also the rail geometry has effect on the inductance gradient.

3
SURROGATE MODELLING

3.1 What is Surrogate Modelling

Product design in engineering is mainly based on a comprehensive analysis of product performance under various design parameters. These analyzes are most often executed through time-consuming computer simulations. A single simulation might take many minutes, hours, or days to complete. Here, surrogate models help us make all these steps easy and feasible. Surrogate modelling is an engineering method used in situations where a result of interest cannot be easily measured directly, so a model of the result is used instead. As a result, recently, a data-based approach called surrogate modeling has been gaining popularity in various fields of engineering since it speeds up routine engineering tasks [47].

3.2 Types of Surrogate Models

There are many surrogate modeling techniques. Some of them are polynomial response surfaces; support vector machines; decision tree based algorithms such as random forests, XGBoost; space mapping; artificial neural networks and Bayesian networks [47].

It is not clear which surrogate model is the most accurate, since the nature of the actual function is not known in advance. And there is no consensus on how to get the most reliable predictions of the accuracy of a given model [47]. For this reason, many surrogate methods should be carried out to find optimum and best solution. The best solution for problems is found by trying and experimenting with various algorithms. For some problems, there is no solution that gives good accuracy, while for some problems, more than one algorithm can give results with high accuracy.

3.2.1 Supervised and Unsupervised Learning

Supervised learning is used when we want to predict a certain result from a certain feature or features. We have a dataset that includes input and outputs. We create a

surrogate model from these input and outputs, that make up our training set. The aim is to make exact predictions for new data that has never been seen before. Supervised learning usually requires manual effort to create the training set, but then it automates the tasks without the need for human labor.

On the other hand, unsupervised learning includes all types of surrogate modeling, in which there is no known output. In unsupervised learning, only input data is shown to the learning algorithm, and it is demanded to get information from these data. [48].

To predict electromagnetic railgun's output force, since the dataset we will create will contain outputs corresponding to certain inputs and train dataset was created by ourselves our case will be supervised learning.

3.2.1.1 Regression and Classification

Supervised problems can be grouped into two classes; one is classification, the other is regression. In classification, the aim is to predict a class label, which is a choice from a predefined list of possibilities. Classification is sometimes divided into binary classification, which is the classification between two classes, and multiclass classification, which is the classification between more than two classes. [48].

For regression tasks, the aim is to estimate a continuous number or a floating-point number in programming terms, or a real number in mathematical terms. Predicting the monthly rent of a house from the number of rooms, size, location and many other critical features is a regression problem. When estimating rent, the estimated value is an amount, and can be any number in a specific range. In order to understand differentiation between classification and regression problem is to ask if there is some kind of continuity in the outcomes. If there is continuity between possible outputs, we can say the problem is a regression problem [48].

Since we want to predict the railgun's electromagnetic force that is continuous number, or a floating-point number from its geometrical inputs, we can say that our case is a regression problem.

3.3 Surrogate Model Techniques Used in This Thesis

Since each algorithm isn't suitable for every problem and we do not know whether the dataset has linear or non-linear attribute, we trained our data with six different techniques to determine the best surrogate model for our dataset.

Used techniques are;

- Artificial Neural Network (ANN)
- Support Vector Regression (SVR)
- Random Forests
- XGBoost
- K Nearest Neighbors (KNN)
- Multiple Linear Regression (MLR)

3.3.1 Artificial Neural Networks

An artificial neural network is a computational model inspired by the structure of neural networks in the brain. In simplified models of the brain, it consists of many basic computing devices which is called neurons interconnected in a complicated communication network, through which the brain can perform quite complicated calculations.

Many neurons can be coupled together by communication links to perform complex calculations. Structure of a neural network can be described as a graph whose nodes are neurons, and each (directed) edge in the graph connects the output of some neuron to the input of another neuron [49].

A neural network structure is given in Figure 3.1 below.

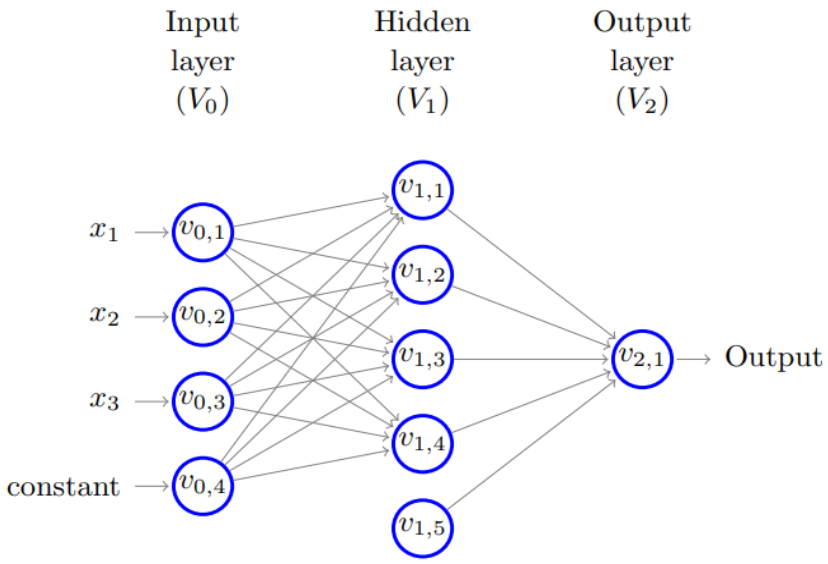


Figure 3.1 An example of neural network structure [49]

The layer on the left, V_0, is called the input layer. It has $n + 1$ neurons, where n is the size of the input space. Layers in the middle are called hidden layers. The layer on the right, is called the output layer. The output layer may consist of one or more neurons depending on the problem. [49].

Neural networks have reemerged as state-of-the-art models in many applications of surrogate modeling. One of their main advantages is that they can capture information contained in a large amount of data and create incredibly complex models. Given enough computation time, data, and careful tuning of the parameters, neural networks often overcome other surrogate modeling techniques for classification and regression tasks. One of the disadvantages of neural networks is that they often take a long time to train, especially large and powerful ones.

In order to get good results from a neural network we have to tune its hyperparameters. Hidden layer size, learning rate, activation function and optimizer are some of the hyperparameters of a neural network to be tuned.

3.3.2 Support Vector Regression

Support Vector Machines (SVMs) are well known in classification problems. The use of SVMs in regression is known as Support Vector Regression. SVR gives us the elasticity to decide how much error is within the limits for our model and finds a

suitable line to fit the data. The error term is instead handled in the constraints, where we set the absolute error less than or equal to a specified margin, called the maximum error, ϵ (epsilon). We can adjust epsilon to achieve the desired accuracy of our model. An illustrative example of SVR is below in Figure 3.2 [50].

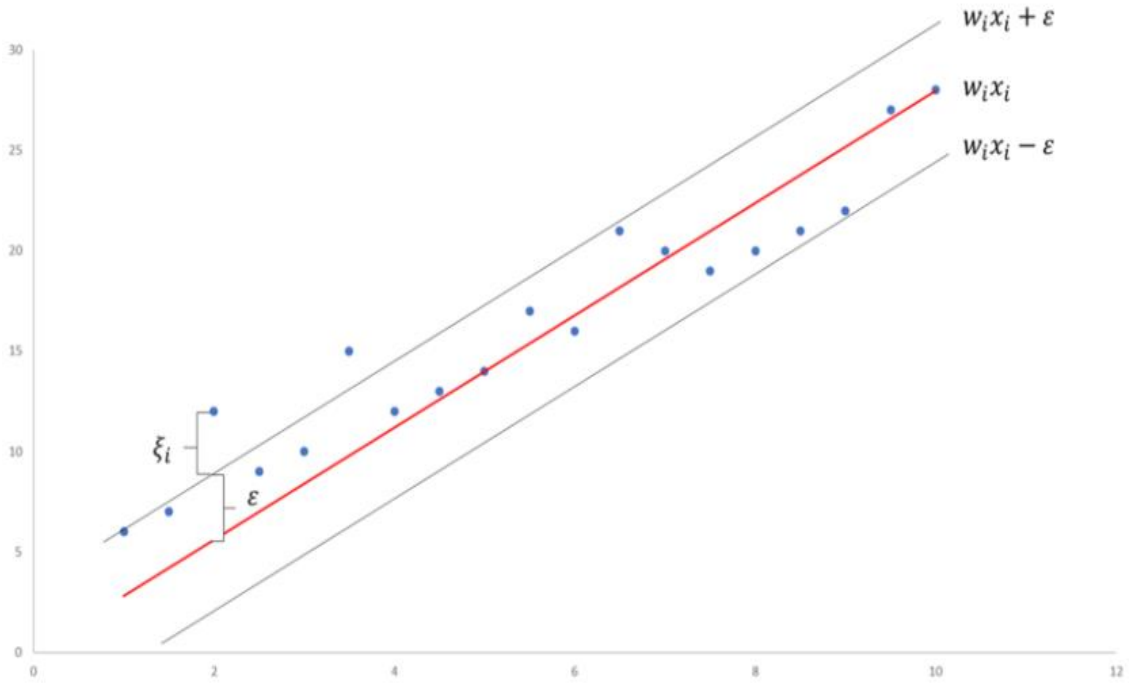


Figure 3.2 Illustrative example of SVR [50]

As it is seen Figure 3.2 some data can be outside of ϵ. We can accurately show its deviation from the margin as ξ. We know that there is a potential for these deviations to exist, but we still want to minimize them as much as possible. Thus, we can add these deviations to objective function of SVR in Equation 3.1 with its constraints in Equation 3.2;

$$\min \frac{1}{2}||w||^2 + C \sum_{i=1}^{n} |\xi_i| \tag{3.1}$$

$$|y_i - w_i x_i| \leq \epsilon + |\xi_i| \tag{3.2}$$

Now we have an additional hyperparameter C. As C increases, the tolerance for points outside of ϵ also increases. As C decreases, the tolerance for points outside of ϵ also decreases. We can say easily that C parameter should be tuned to get a better

model and SVR is a strong algorithm that provides us to choose how tolerant we are of errors, both through an acceptable error margin(ϵ) and through tuning our tolerance of falling outside that acceptable error rate [50].

3.3.3 Random Forests

Random Forests is a decision tree algorithm. It is used in both regression and classification problems. Mainly, they learn a hierarchy of if/else questions, driving to a decision. Each tree can make relatively good job of predicting, but will likely overfit on part of the data. If a large number of trees are built that all work well and are overfit in different ways, overfitting can be reduced by averaging their results. Random forests algorithm solves this overfit problem this way, which is the main problem of the decision tree algorithm. [48].

An important hyperparameter of random forests is max_features. If we set max_features to feature numbers of the train set, each split looks at all features in the dataset, and we lose randomness here. On the other hand, if max_features are set to 1, the splits have no choice at all on which feature to test, and can only search at different thresholds for the randomly selected feature. For this reason, we have to tune the max_features parameter in order not to get trees in random forests that are too similar or too different from each other. [48].

3.3.4 XGBoost

The XGBoost is an optimized distributed gradient boosting library designed to be highly productive, elastic and portable. It implements surrogate modeling algorithms under the Gradient Boosting framework. XGBoost provides a parallel tree that solve many real-world problems in a fast and accurate way [51].

XGBoost can be used not only in regression but also used in classification problems. On the contrary the random forest algorithm, gradient boosting works by building trees in a serial way, where each tree tries to correct the errors of the previous tree. Gradient boosted trees reduce the memory usage during the training and makes predictions faster. Gradient boosting combines many simple models; each tree provides good predictions on part of the data, and so more and more trees are added to iteratively improve performance. According to the random forests Gradient

boosting sensitive to parameter settings but can provide better accuracy if the parameters are tuned rightly. An important hyperparameter of XGBoost is learning rate, which controls how strongly each tree tries to correct the errors of the previous trees. A higher learning rate means that each tree can make stronger corrections and allow for more complex models. By increasing n_estimators parameter adding more trees to the group increases the model complexity, as the model has more chances to correct errors on the training set [48].

3.3.5 K-Nearest Neighbors

The KNN is the simplest and easy to understand algorithm beyond dispute. Preparing a training and test dataset is enough to create a surrogate model. The algorithm finds the nearest data points to make a prediction for a new data point in the training dataset its "nearest neighbors."

Building the nearest neighbors model is usually very fast. If the training set is very large prediction can be slow. Advantages of the KNN are that the model is very easy to understand, parameter tuning and training is easy. It gives good performance without a lot of tunning. KNN is a good start point before more advanced and complicated modeling techniques [48].

There are two important hyperparameters of the KNN, these are; the number of neighbors and distance measurement method between the data points [48].

3.3.6 Multi Linear Regression

Linear regression tries to find a linear relation between the input features and the output of the dataset. This linear relationship symbolized by a linear function. Linear models make predictions using this linear function. If a dependent variable is explained by only one variable, it is called linear regression. But if a dependent variable is explained more than one independent variable it is called multiple linear regression. For linear regression, the general formula can be written as:

$$\hat{y} = w[0] * x[0] + w[1] * x[1] + ... + w[p] * x[p] + b \quad (3.3)$$

Here, x[0] to x[p] indicate the input features. In this problem, the number of input features is p. w and b are the coefficients that the model is trying to learn, and $\hat{y}$ is

the predicted value [48]. In Equation 3.3, since $\hat{y}$ depends on more than one independent variable, we can say this is a Multi Linear Regression problem.

Linear regression finds the w and b that minimize the mean squared error between predictions and the targets. Linear regression has no hyperparameters to tune, it seems this is a benefit, but this is a drawback actually, we cannot control the model complexity for this reason [48].

4
RAILGUN'S ELECTROMAGNETIC FORCE USING SURROGATE MODELLING TECHNIQUES

Artificial Intelligence based surrogate model is a concept that allows the machine to learn from data and experiences with using algorithms. These models gain the ability to prediction and classify by examining and learning the previous cases [49]. That's why surrogate models can predict or classify new cases with very high accuracy and easily.

Half-cylindrical rail - C type armature pair was selected for AI based surrogate modelling. This pair's geometric variables are shown in Figure 4.1 This model was analyzed with the geometric values that are given in the Table 4.1 According to the variables in the Table 4.1, 486 combinations were created. Therefore, 486 independent simulations were carried out. Simulation results were saved to create train and test dataset for the surrogate models.

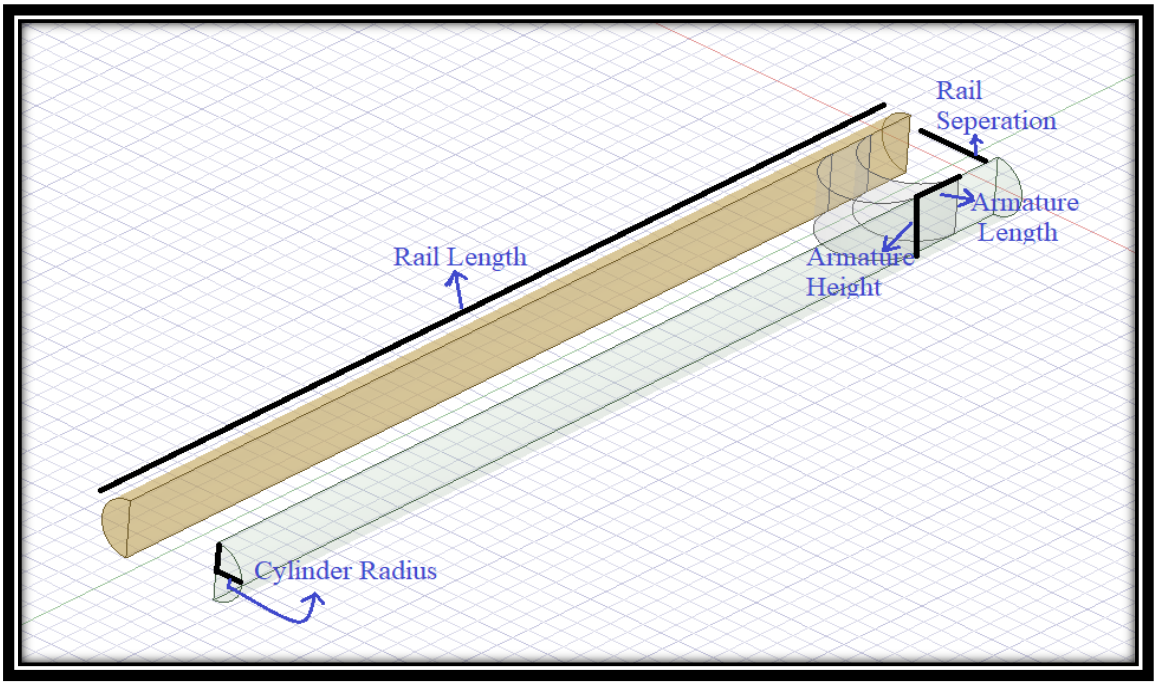


Figure 4.1 Railgun geometric variables

Table 4.1 Geometric variables and dataset inputs

Input parameters	Values [cm]
Rail Length (Rail_L)	100 - 150 - 200
Rail Separation (Seperation)	5 -10 -15
Cylinder Radius (Cyl_Rad)	1 - 3 - 5
Armature Length (Arm_L)	1 - 3- 5
Armature Height (Arm_H)	1 - 3- 5 - 7 - 9 - 11
Total number of combinations	486

Dataset was divided by 0.25 test data and 0.75 train data. Some examples of the dataset are given in Table 4.2 After model tuning, surrogate models that is mentioned in the previous section were trained and tested using Keras and Scikit-Learn frameworks on Python 3.7 environment.

Table 4.2 Some examples of dataset

Armature height [cm]	Armature length [cm]	Cylinder radius [cm]	Rail length [cm]	Rail separation [cm]	Output force (kNewton)
7	1	5	100	5	2.23
11	5	3	150	15	4.08
9	3	5	200	10	2.84

The output force predictions of railguns whose dimensions are not within the trained models' dimension range will not be correct. For example, accurate predictions will not be obtained for rail lengths of more than 200 cm, less than 100 cm or armature height of more than 11 cm, less than 1 cm. Therefore, the output force predictions of the model will be within the limits of the trained data. If the user wants predictions in a wider or tight range, the train data should be created in this scope of range as well.

Used models, model tuning parameters and best parameters are given in Table 4.3. When model tuning stage, it is difficult to manually change the hyper parameters. Therefore, GridSearchCV method was used. GridSearchCV is a sklearn's library function. With this method, training was carried out by cross-matching with all hyperparameters that is wanted to be combine each other. Then the parameters which we get the best result were added to the best parameter column in the Table 4.3.

In all methods, input data was normalized using the minimum and maximum value of input data as given in Equation 4.1. The normalized data was given as input to model for prediction.

In order to evaluate surrogate model accuracy, there are many measurement techniques. In this study root mean square error (RMSE) as given in Equation 4.2 [52] and symmetric mean absolute percentage error (SMAPE) as given in Equation 4.3 [52] were used for model evaluation.

$$y' = \frac{y - min_y}{max_y - min_y} \tag{4.1}$$

$$RMSE = \sqrt{\frac{1}{n}\sum_{j=1}^{n}\left(y_j - \hat{y}_j\right)^2} \tag{4.2}$$

$$SMAPE = \frac{1}{n}\sum_{j=1}^{n}\frac{100 * \left|y_j - \hat{y}_j\right|}{\left(\left|y_j\right| + \left|\hat{y}_j\right|\right)/2} \tag{4.3}$$

Where y' normalized input, y_j, $\hat{y}_j$ are target and predicted values and n is the number of samples respectively.

Table 4.3. Model tuning parameters

Model	**Used parameters for model tuning with GridSearchCV method**	**Best parameters**
ANN	cross validation: 5 estimator = MLPRegressor activation functions : 'identity', 'logistic', 'tanh', 'relu','elu', 'selu', 'exponantial' Epochs:500 Learning rate: 0,001 early_stopping: True hidden_layer_sizes: 10, 15, 20, 30, (10, 15), (15, 20), (20, 20), (20, 30), (60, 90), (100, 20) (10, 15, 20), (15, 20, 30), (20, 20, 20), (50, 50, 50), (30, 90, 120), (120, 90, 30), (100, 50, 150), (300, 200, 150) dropout: 0.2, 0.3, 0.5, False optimizer: 'SGD', 'RMSprop', 'Adagrad', 'Adadelta', 'Adam', 'Ftrl', 'Adamax', 'Nadam'	Activation func: 'relu', hidden_layer_size: (300, 200, 150), Dropout: False, optimizer: 'Adam'
SVR	cross validation: 5, estimator= SVR (cache_size=200, coef0=0.0, degree=3, epsilon=0.1, gamma='scale', kernel='rbf', max_iter=-1, shrinking=True, tol=0.001), 'C': [0.1, 0.4, 3, 5, 20, 10000, 20000, 100000]	Regularization parameter (C): 10000

Table 4.3. Model tuning parameters (continued)

Random Forests	cross validation: 5, estimator = RandomForestRegressor (bootstrap=True, ccp_alpha=0.0, criterion='mse', max_depth=None, max_features='auto', max_leaf_nodes=None, max_samples=None, min_impurity_decrease=0.0 min_impurity_split=None, min_samples_leaf=1, min_samples_split=2, min_weight_fraction_leaf=0) 'max_depth': [1, 2, 3, 4, 5, 6, 7, 8, 9], 'max_features': [2, 3, 4,5], 'n_estimators': [50, 100, 200, 500, 1000, 2000]}	max_depth : 8, max_features : 4, n_estimators : 2000

Table 4.3. Model tuning parameters (continued)

KNN	cross validation=5, estimator = KNeighborsRegressor (algorithm='auto', leaf_size=30, metric='minkowski', metric_params=None n_neighbors=5, p=2, weights='uniform'), 'n_neighbors': [1, 2, 3, 4, 5, 6, 7, 8, 9, 10, 11, 12, 13, 14, 15, 16, 17, 18, 19, 20, 21, 22, 23, 24, 25, 26, 27, 28, 29]	n_neighbors: 5
MLR	Method : Least Squares LinearRegression (fit_intercept=True) There are no parameters to tune	Method : Least Squares LinearRegression (fit_intercept: True)

Table 4.3. Model tuning parameters (continued)

XGBoost	cross validation=5, estimator = XGBRegressor(base_score=None, booster=None, colsample_bylevel=None, colsample_bynode=None, colsample_bytree=None, gamma=None, missing=nan, importance_type='gain', interaction_constraints=None, learning_rate=None, max_delta_step=None, max_depth=None, min_child_weight=None, monotone_constraints=None, reg_lambda=None, scale_pos_weight=None, subsample=None, tree_method=None, validate_parameters=None, 'colsample_bytree': [0.4, 0.5, 0.7, 0.9, 1], 'learning_rate': [0.001, 0.01, 0.1, 0.2, 0.5] 'max_depth': [2, 3, 4, 5, 8], 'n_estimators': [100, 200, 500, 1000]	colsample_bytree : 0.7, learning_rate: 0.1, max_depth: 3, n_estimators: 1000

Prediction results are shown in Table 4.4. Since ANN and Random Forests models' outputs change with every model fitting, 10 independent fitting were carried out for these models and their averages were given with their standard deviations.

Besides, to compare predictions of the best and the worst surrogate model, prediction graphs were given in Figure 4.2 - Figure 4.7. Test data (0.25 of entire dataset) was used as target data in mentioned predictions.

Table 4.4 Prediction results

Model	**SMAPE**	**RMSE**
Artificial Neural Network (ANN)	average: 1.89 std.dev:0.05	average: 0.126 std.dev:0.001
Support Vector Regression (SVR)	3.57	0.2
Random Forests	average: 2.37 std.dev:0.06	average: 0.175 std.dev:0.003
K Nearest Neighborhood (KNN)	7.21	0.412
Multiple Linear Regression	11.44	2.03
XGBoost	1.96	0.1347

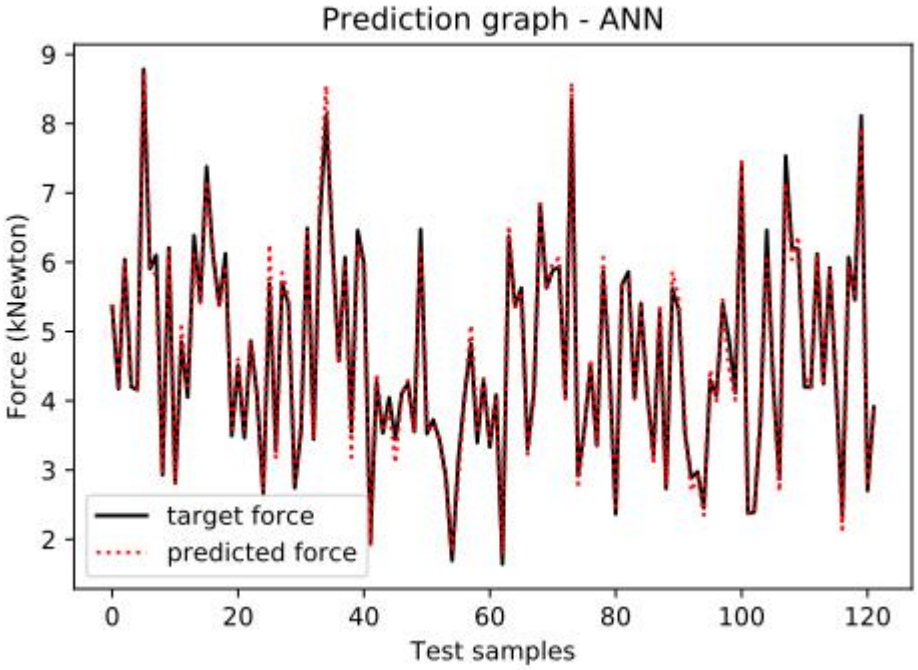


Figure 4.2 Prediction graph of ANN method

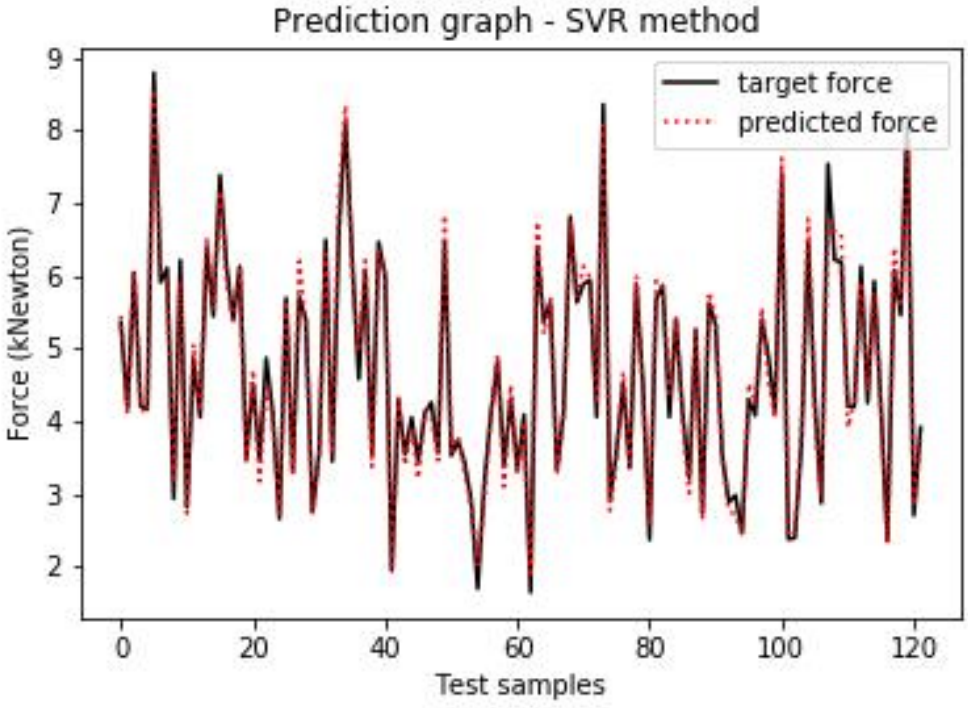


Figure 4.3 Prediction graph of SVR method

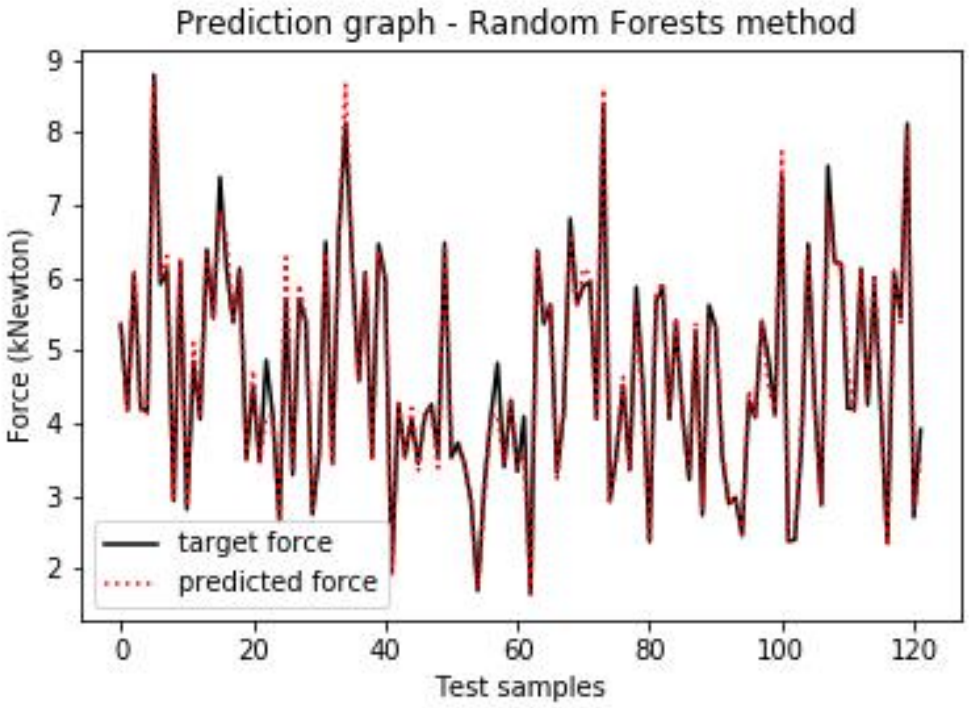


Figure 4.4 Prediction graph of Random Forests method

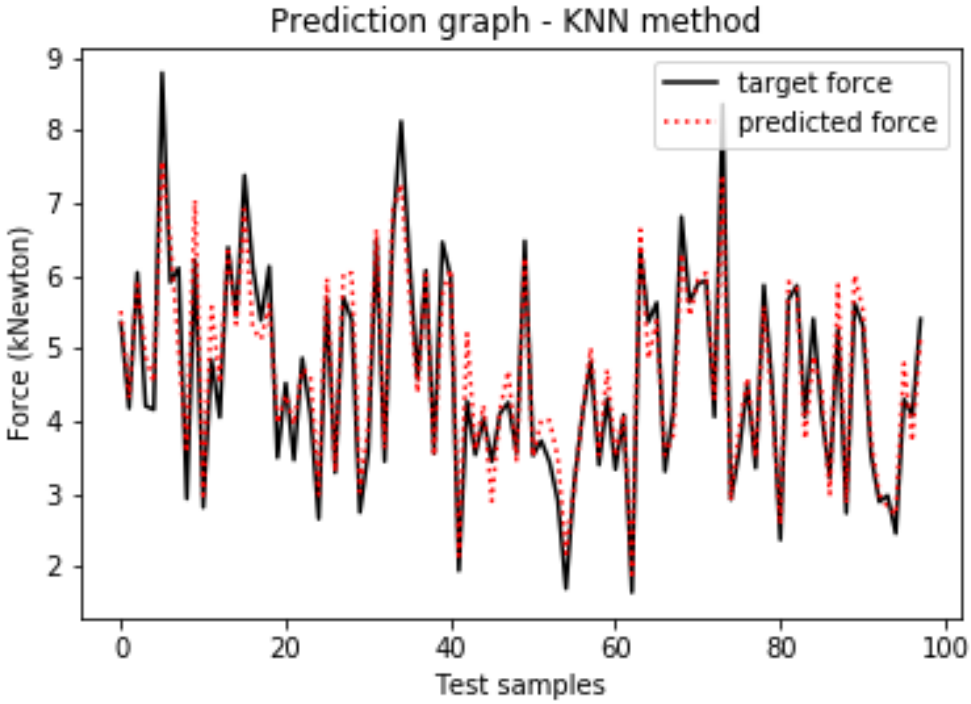


Figure 4.5 Prediction graph of KNN method

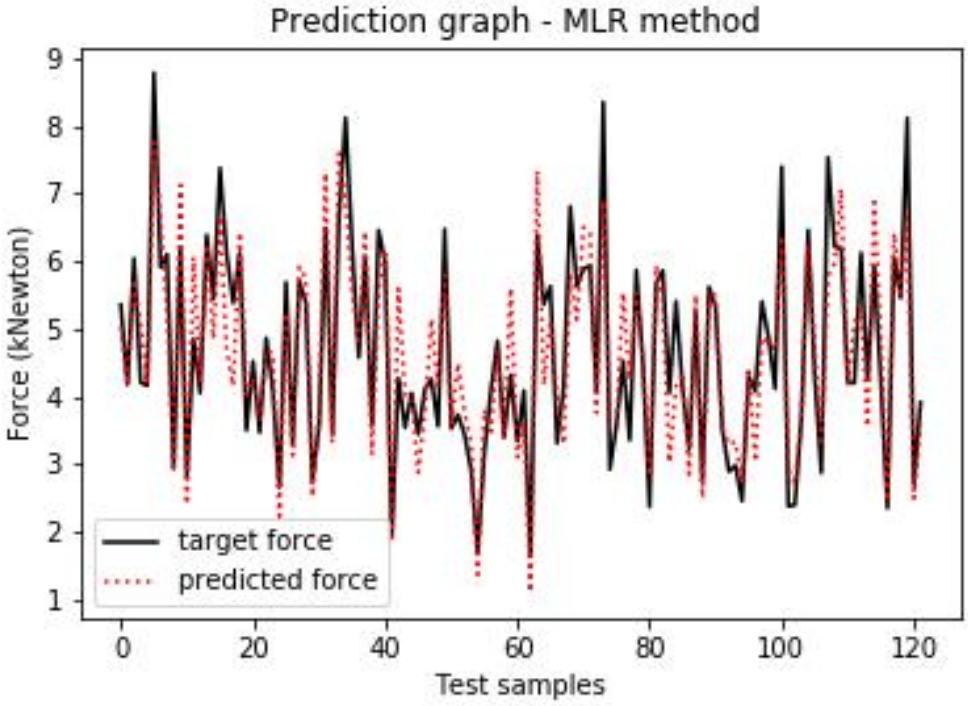


Figure 4.6 Prediction graph of MLR method

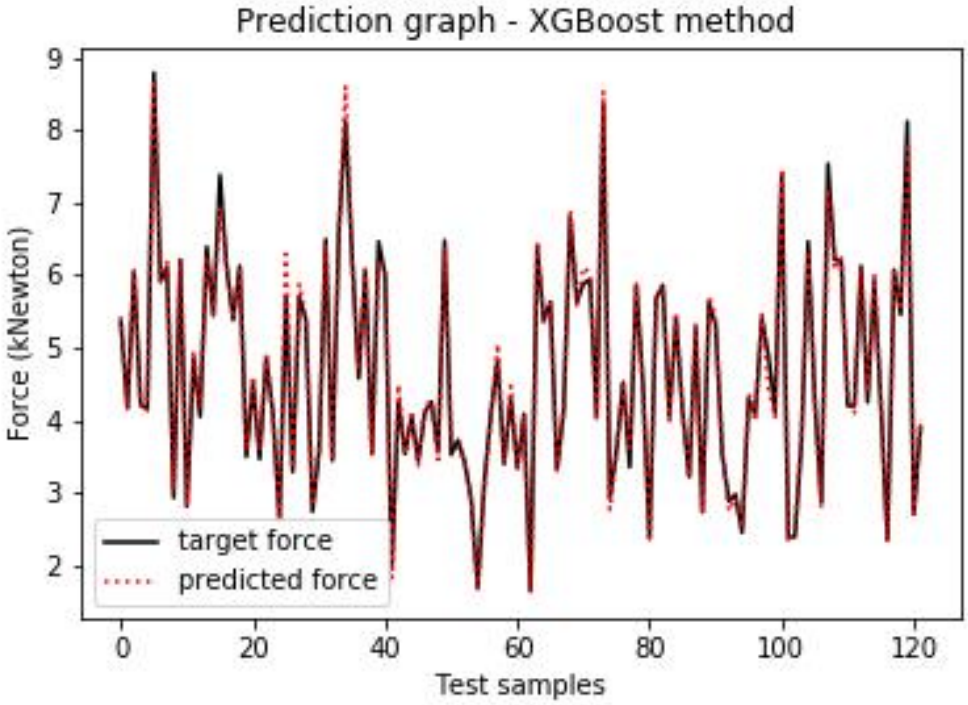


Figure 4.7 Prediction graph of XGBoost method

5
PARTICLE SWARM OPTIMIZATION

PSO is one of the commonly used traditional optimization algorithm, has been used in the Matlab environment for a selected cost function. In the last decades, MHA has been widely used as an powerful solution method for finding optimal solutions in design optimization tasks of many microwave devices [21-32] as well. Due to their unique heuristic search methods, these algorithms can be used in for solving non-differentiable or discontinuous, non-convex problems. Also, they are used for solving nonlinear problems that might not be solved with gradient based algorithms [3].

PSO algorithm tries to reach the optimum point by minimizing the cost function. Input parameters that create the predicted force are continuous in the optimization process, it doesn't have to be discrete as it is seen in Table 5.1.

Used cost function is given in Equation 5.1 below:

$$C = |required\ force - predicted\ force| \tag{5.1}$$

In the dataset that we use for this model, railgun's output force range is between 1.62 kNewton and 9.54 kNewton. For this reason, while performing PSO optimization, this range was not exceeded. This optimization is able to work in this range, but we just optimized only 8.0 kNewton for the sample in the study.

Required inputs for 8.0 kNewton required output force were found using PSO algorithm with 30, 50, 100 populations. Moreover, number of iterations were examined to see the convergency of the algorithm. Optimization results have been compared with Ansys outputs in Table 5.1 as well. As seen in Table 5.1; at first, PSO reached 7.99 kNewton with 30 population and 10 iterations, after this point increasing the population size did not change the result but increasing the iterations to 30 converged the result to 8.0 kNewton.

Table 5.1 Optimization results

Input Optimization with Partical Swarm Optimization (PSO) for 8.0 kNewton Output Force							
Iteration / Population	**Inputs [cm]**					**PSO result (kN)**	**Ansys result (kN)**
	Arm_H	**Arm_L**	**Cyl_Rad.**	**Rail_L**	**Seperation**		
10 / 30	1	5	1	142	12.7	7.99	7.93
10 / 50	1	1	1	100	7	7.99	8.06
10 / 100	1	5	1	100	14.4	7.99	7.98
30 / 30	1	5	1	200	10.5	8	8.07
30 / 50	1	5	1	100	14.4	8	7.98
30 / 100	1	5	1	200	10.5	8	8.07
50 / 30	1	5	1	200	10.5	8	8.07
50 / 50	1	5	1	100	14.4	8	7.98
50 / 100	1	5	1	200	10.5	8	8.07

6
RESULTS AND DISCUSSION

We simulated and analyzed the three rails geometry and the three types of armatures to obtain high inductance gradient for achieving higher output force and so higher projectile velocities.

Simulation results show that C type armature provides best inductance gradient with all type of rails. Although the volume of the armature is not effective on the output force, it was seen that the surface area of the armature is effective. While C type armature with high surface area has given better performance in all situations, rectangular and hollow type armatures with low surface area has given lower and almost same performance as each other.

Results validate that there is a dependency between the effectiveness of railgun and its geometry. After creating a dataset, railgun electromagnetic force can be predicted with the surrogate model algorithms easily, without the need to repeatedly draw and simulate.

Surrogate model prediction results show that Artificial Neural Network, XGBoosts and Random Forests methods are very successful for our dataset. They achieved railgun electromagnetic output force prediction with minimum SMAPE of 1.89%, 1.96% and 2.37% respectively.

Also, PSO showed that we can easily determine the railgun geometry inputs to get the desired output force. In this way; quick, easy and low-cost analyses can be done before production.

Further analysis on the effects of hyper parameters was not studied in this work since the proposed method already achieved acceptable results. However, in future works for design problems with higher non-linearity characteristics between inputs and outputs alongside a wider range of variables, optimization and optimal

determination of hyper-parameters for surrogate model is a must and will be taken into the consideration in future works.

REFERENCES

[1] R. Murugan and K. Udayakumar, "Effect of Rail Dimensions on Rail Gun Design Parameters," 2005 Annual IEEE India Conference - Indicon, 2005, pp. 623-626, doi: 10.1109/INDCON.2005.1590247.

[2] P. Mahouti, "Application of artificial intelligence algorithms on modeling of reflection phase characteristics of a nonuniform reflectarray element," International Journal of Numerical Modelling: Electronic Networks, Devices and Fields, vol. 33, no. 2, 2020, doi:10.1002/jnm.2689.

[3] P. Mahouti, "Design optimization of a pattern reconfigurable microstrip antenna using differential evolution and 3D EM simulation-based neural network model," International Journal of RF and Microwave Computer-Aided Engineering, vol. 29, no. 8, 2019, doi: 10.1002/mmce.21796.

[4] F. Giannini, G. Leuzzi, G. Orengo and M. Albertini, "Small-signal and large-signal modeling of active devices using CAD-optimized neural networks," International Journal of Rf and Microwave Computer-aided Engineering, vol. 12, no. 1, pp. 71-78, 2002, doi: 10.1002/mmce.10007.

[5] Z. Marinković, and V. Markovic, "Temperature-dependent models of low-noise microwave transistors based on neural networks," International Journal of Rf and Microwave Computer-aided Engineering, vol. 15, no. 6, pp. 567-57, 2005, doi: 10.1002/mmce.20102.

[6] F. Güneş, P. Mahouti, S. Demirel, M.A. Belen and A. Uluslu, "Cost-effective GRNN-based modeling of microwave transistors with a reduced number of measurements," International Journal of Numerical Modelling-electronic Networks Devices and Fields, vol. 30, 2017, doi: 10.1002/jnm.2089.

[7] M.A., Belen, F. Güneş, P. Mahouti and S. Demirel, "Signal and Noise Modeling of Microwave Transistors Using Characteristic Support Vector-based Sparse Regression," Radioengineering, vol. 25, no. 3, pp. 490-499, 2016, doi: 10.13164/re.2016.0490.

[8] Z. Marinković, G. Crupi, A. Caddemi, V. Markovic and D. Schreurs, "A review on the artificial neural network applications for small-signal modeling of microwave FETs," International Journal of Numerical Modelling-electronic Networks Devices and Fields, vol. 33, no. 3, 2019, doi: 10.1002/jnm.2668.

[9] F. Güneş, S. Demirel, and P. Mahouti, "Design of a Front-End Amplifier for the Maximum Power Delivery and Required Noise by HBMO with Support Vector Microstrip Model," Radioengineering, vol. 29, no. 1, pp. 4–20, 2015, doi: 10.1002/jnm.2041.

[10] F. Güneş, S. Demirel and S. Nesil, "A Novel Design Approach to X-Band Minkowski Reflectarray Antennas using the Full-Wave EM Simulation-based Complete Neural Model with a Hybrid GA-NM Algorithm," Radioengineering, vol. 23, no.1, pp. 144-153, 2014.

[11] P. Mahouti, F. Güneş, M.A. Belen and A. Çalışkan, “A Novel Design of Non-Uniform Reflectarrays with Symbolic Regression and its Realization using 3-D Printer,” Aces Journal, vol. 34, no. 2, pp. 280-285, 2019, doi: 10.1002/jnm.2746.

[12] M. Mahouti, N. Kuskonmaz, P. Mahouti, M.A. Belen, and M. Palandoken, “Artificial neural network application for novel 3D printed nonuniform ceramic reflectarray antenna,” International Journal of Numerical Modelling-electronic Networks Devices and Fields, vol. 33, no. 6, 2020, doi: 10.1002/jnm.2746.

[13] J. Lakshmi Narayana, K. Sri Rama Krishna and L. Pratap Reddy, "ANN models for coplanar strip line analysis and synthesis," 2008 International Conference on Recent Advances in Microwave Theory and Applications, 2008, pp. 682-685, doi: 10.1109/AMTA.2008.4762991.

[14] P. Mahouti, F. Gunes, M.A. Belen and S. Demirel, “Symbolic Regression for Derivation of an Accurate Analytical Formulation Using Big Data: An Application Example,” Applied Computational Electromagnetics Society Journal, vol. 32, no: 5, pp. 372-380, May 2017.

[15] D. Karaboga, K. Güney, S. Sagiroglu and M. Erler, “Neural computation of resonant frequency of electrically thin and thick rectangular microstrip antennas,” IEEE Proc Microwave Antennas Propagation, vol. 146, no: 2, pp. 155-159, 1999, doi: 10.1049/ip-map:19990136

[16] R. K. Mishra and A. Patnaik, "Neural network-based CAD model for the design of square-patch antennas," in IEEE Transactions on Antennas and Propagation, vol. 46, no. 12, pp. 1890-1891, Dec. 1998, doi: 10.1109/8.743842.

[17] N. Çalik, M.A. Belen, and P. Mahouti, “Deep learning base modified MLP model for precise scattering parameter prediction of capacitive feed antenna,” International Journal of Numerical Modelling-electronic Networks Devices and Fields, vol. 33, no. 5, 2020, doi: 10.1002/jnm.2682

[18] S. Metlek, K. Kayaalp, I. Basyigit, A. Genc and H. Dogan, “The dielectric properties prediction of the vegetation depending on the moisture content using the deep neural network model,” International Journal of Rf and Microwave Computer-aided Engineering, vol. 31, no. 1, pp. 1-10, 2021, doi: 10.1002/mmce.22496.

[19] I. Basyigit and H. Dogan, “The Analytical and Artificial Intelligence Methods to Investigate the Effects of Aperture Dimension Ratio on Electrical Shielding Effectiveness,” International Journal of Electronics and Telecommunications, vol. 65, no. 3, pp. 359-365, 2019, doi: 10.24425/ijet.2019.126322.

[20] I. Basyigit, A. Genc, H. Dogan, F.A. Şenel and S. Helhel, “Deep learning for both broadband prediction of the radiated emission from heatsinks and heatsink optimization,” Engineering Science and Technology, an International Journal, vol. 24, no. 6, pp. 706-714, 2021, doi: 10.1016/j.jestch.2021.01.006

[21] F. Güneş, S. Demirel and P. Mahouti, “A simple and efficient honey bee mating optimization approach to performance characterization of a microwave transistor for the maximum power delivery and required noise,” International Journal of Numerical Modelling-electronic Networks Devices and Fields, vol. 29, no. 1 pp. 4-20, Jan 2015, doi: 10.1002/jnm.2041.

[22] F. Güneş, S. Demirel and P. Mahouti, “Design of a Front-End Amplifier for the Maximum Power Delivery and Required Noise by HBMO with Support Vector Microstrip Model,” International Journal of Numerical Modelling: Electronic Networks, Devices and Fields, vol. 29, no. 1, pp. 4-20, 2014, doi: 10.1002/jnm.2041.

[23] S. Y. Zheng, "The applications of jumping genes inspired evolutionary algorithms in microwave circuit designs," 2017 International Applied Computational Electromagnetics Society Symposium (ACES), 2017, pp. 1-2.

[24] K. Guney, and M. Onay, “Bees algorithm for design of dual-beam linear antenna arrays with digital attenuators and digital phase shifters,” International Journal of Rf and Microwave Computer-aided Engineering, vol. 18, no. 4, pp. 337-347, July 2008, doi: 10.1002/mmce.20292.

[25] A. Galehdar, D. Thiel, A. Lewis, and M. Randall, “Multiobjective optimization for small meander wire dipole antennas in a fixed area using ant colony system,” International Journal of Rf and Microwave Computer-aided Engineering, vol. 19, no. 5, pp. 592-597, 2009, doi: 10.1002/mmce.20382.

[26] S. Y. Zheng, S. H. Yeung, W. S. Chan, K. F. Man and K. S. Tang, "Design of Broadband Hybrid Coupler With Tight Coupling Using Jumping Gene Evolutionary Algorithm," in IEEE Transactions on Industrial Electronics, vol. 56, no. 8, pp. 2987-2991, Aug. 2009, doi: 10.1109/TIE.2009.2020080.

[27] F. Güneş, M.A. Belen and P. Mahouti, “Competitive evolutionary algorithms for building performance database of a microwave transistor,” Int. J. Circuit Theory Appl., vol. 46, no. 2, pp. 244-258, 2018, doi: 10.1002/cta.2386.

[28] A. Yıldırım, F. Güneş, and M.A. Belen, “Differential Evolution Optimization Applied to the Performance Analysis of a Microwave Transistor. Sigma J. Eng & Nat Sci, vol. 8, no. 2, pp. 135-144, 2017.

[29] H. Clark, N. S. Jeong and S. Jeong, "Concurrent Gain and Bandwidth Improvement of a Patch Antenna with a Hybrid Particle Swarm Optimization Algorithm," 2019 IEEE 20th Wireless and Microwave Technology Conference (WAMICON), 2019, pp. 1-3, doi: 10.1109/WAMICON.2019.8765432.

[30] Y. Rahmat-Samii, "Modern Antenna Designs using Nature Inspired Optimization Techniques: Let Darwin and the bees help designing your Multi band MIMO antennas," 2007 IEEE Radio and Wireless Symposium, 2007, pp. 463-466, doi: 10.1109/RWS.2007.351868.

[31] P. Patel, G. Kumari and P. Saxena, "Array Pattern Correction in Presence of Antenna Failures using Metaheuristic Optimization Algorithms," 2019 International Conference on Communication and Signal Processing (ICCSP), 2019, pp. 0695-0700, doi: 10.1109/ICCSP.2019.8697942.

[32] N. S. Grewal, M. Rattan and M. S. Patterh, "A linear antenna array failure detection using Bat Algorithm," 2015 Eighth International Conference on Contemporary Computing (IC3), 2015, pp. 202-207, doi: 10.1109/IC3.2015.7346679.

[33] Y. Çevik, “Modeling of an Electromagnetic Launcher,” M.Sc. Thesis, METU, Turkey, 2015.

[34] A. Weedon, “What exactly is a railgun, and do we need to start building bunkers again?,” *ABC News*, 04-Jan-2019. [Online]. Available: https://www.abc.net.au/news/2019-01-03/the-railgun-explained-and-what-it-means-for-us-china-relations/10683526. [Accessed: 13-Feb-2022].

[35] A. S. Feliciano, “The Design and Optimization of a Power Supply for a One meter Electromagnetic Railgun,” Master’s thesis, Naval Postgraduate School, Monterey, California, December 2001.

[36] “Railgun,” *Wikipedia,* 17-Jan-2022. [Online]. Available: https://en.wikipedia.org/wiki/Railgun. [Accessed: 13-Feb-2022].

[37] J. Kerrisk, “Current distribution and inductance calculations for rail-gun conductors,” United States, 1981.

[38] R. A. Marshall, "Railgun bore geometry, round or square?," in IEEE Transactions on Magnetics, vol. 35, no. 1, pp. 427-431, Jan. 1999, doi: 10.1109/20.738445.

[39] Z. Yadong, R. Jiang-jun, H. Yuanchao, G. Ruohan and W. Wu, “Ablation and geometry change study of solid armature in a railgun,” Chinese Physics B, vol. 22, no. 8, 2013, doi: 10.1088/1674-1056/22/8/084102.

[40] A. Keshtkar, S. Bayati and A. Keshtkar, "Effect of Rail's Material on Railgun Inductance Gradient and Losses," 2008 14th Symposium on Electromagnetic Launch Technology, 2008, pp. 1-4, doi: 10.1109/ELT.2008.33.

[41] N. Tosun, “Transient Modeling Techniques for the Analysis of Electromagnetic Launchers,” M.Sc. Thesis, METU, Turkey, 2021.

[42] Bok-Ki Kim and Kuo-Ta Hsieh, "Effect of rail/armature geometry on current density distribution and inductance gradient," in IEEE Transactions on Magnetics, vol. 35, no. 1, pp. 413-416, Jan. 1999, doi: 10.1109/20.738442.

[43] L. Chen, J. He, S. Xia, Z. Yuan and H. He, "Some Key Parameters of Monolithic C-Type Armature in Rectangular Caliber Railgun," in IEEE Transactions on Plasma Science, vol. 45, no. 7, pp. 1465-1469, July 2017, doi: 10.1109/TPS.2017.2705702.

[44] C. Du, “Analysis of Materials Selection for Electromagnetic Railguns,” 5th International Conference on Machinery, Materials and Computing Technology, Advances in Engineering, vol. 126, Jan 2017, doi: 10.2991/icmmct-17.2017.42.

[45] P. Zuo, J. Li, X. Song and J. Yuan, "Characteristics of the Current Distribution in Rails and Armature with Different Section Shape Rails," 2012 16th International Symposium on Electromagnetic Launch Technology, 2012, pp. 1-6, doi: 10.1109/EML.2012.6325127.

[46] Y. Xing, Q. Lv, B. Lei, H. Xiang, R. Zhu and C. Liu, "Analysis of Transient Current Distribution in Copper Strips of Different Structures for Electromagnetic Railgun," in IEEE Transactions on Plasma Science, vol. 43, no. 5, pp. 1566-1571, May 2015, doi: 10.1109/TPS.2015.2414095.

[47] “Surrogate model,” *Wikipedia,* 25-Jan-2022. [Online]. Available: https://en.wikipedia.org/wiki/Surrogate_model. [Accessed: 13-Feb-2022].

[48] A. C. Müller and S. Guido, *Introduction to machine learning with python: A guide for data scientists*. Sebastopol: O'Reilly Media, 2018.

[49] S. Shalev-Shwartz and S. Ben-David, *Understanding machine learning: From theory to algorithms*. Cambridge: Cambridge University Press, 2021.

[50] T. Sharp. "An introduction to support vector regression (SVR)," *Medium*, 06-May-2020. [Online]. Available: https://towardsdatascience.com/an-introduction-to-support-vector-regression-svr-a3ebc1672c2. [Accessed: 13-Feb-2022].

[51] "XGBoost documentation¶," *XGBoost Documentation - xgboost 1.5.2 documentation*.[Online].Available: https://xgboost.readthedocs.io/en/stable [Accessed:13-Feb-2022].

[52] R. Hyndman and A. Koehler, "Another look at measures of forecast accuracy," International Journal of Forecasting, vol. 22, no. 4, pp. 679-688, 2006, doi: 10.1016/j.ijforecast.2006.03.001.

PUBLICATIONS FROM THE THESIS

Papers

1. H.A. Akyol and A. Kızılay, "Design Optimization of Railgun's Electromagnetic Force Using Surrogate Modelling Techniques," Sigma Journal of Engineering and Natural Sciences, Mart 2022.